Subscriber access provided by CORNELL UNIVERSITY LIBRARY

Article

Electronic Asymmetry of an Annellated Pyridyl–Mesoionic Carbene Scaffold: Application in Pd(II) Catalyzed Wacker#type Oxidation of Olefins

Sayantani Saha, suman yadav, Noor U Din Reshi, Indranil Dutta, Sooraj Kunnikuruvan, and Jitendra K. Bera

ACS Catal., **Just Accepted Manuscript** • DOI: 10.1021/acscatal.0c02729 • Publication Date (Web): 08 Sep 2020

Downloaded from pubs.acs.org on September 8, 2020

Just Accepted

"Just Accepted" manuscripts have been peer-reviewed and accepted for publication. They are posted online prior to technical editing, formatting for publication and author proofing. The American Chemical Society provides "Just Accepted" as a service to the research community to expedite the dissemination of scientific material as soon as possible after acceptance. "Just Accepted" manuscripts appear in full in PDF format accompanied by an HTML abstract. "Just Accepted" manuscripts have been fully peer reviewed, but should not be considered the official version of record. They are citable by the Digital Object Identifier (DOI®). "Just Accepted" is an optional service offered to authors. Therefore, the "Just Accepted" Web site may not include all articles that will be published in the journal. After a manuscript is technically edited and formatted, it will be removed from the "Just Accepted" Web site and published as an ASAP article. Note that technical editing may introduce minor changes to the manuscript text and/or graphics which could affect content, and all legal disclaimers and ethical guidelines that apply to the journal pertain. ACS cannot be held responsible for errors or consequences arising from the use of information contained in these "Just Accepted" manuscripts.

is published by the American Chemical Society. 1155 Sixteenth Street N.W.,
Washington, DC 20036

Published by American Chemical Society. Copyright © American Chemical Society.
However, no copyright claim is made to original U.S. Government works, or works produced by employees of any Commonwealth realm Crown government in the course of their duties.

Electronic Asymmetry of an Annellated Pyridyl–Mesoionic Carbene Scaffold: Application in Pd(II) Catalyzed Wacker–type Oxidation of Olefins

*Sayantani Saha, Suman Yadav, Noor U Din Reshi, Indranil Dutta, Sooraj Kunnikuruvan and Jitendra K. Bera**

**Department of Chemistry and Center for Environmental Science, Indian Institute of Technology Kanpur, Kanpur, 208016, India*

ABSTRACT

The two donor modules of an annellated pyridyl–mesoionic carbene ligand (aPmic) have different σ– and π–bonding characteristics leading to its electronic asymmetry. A Pd(II) complex **1** featuring aPmic catalyzes the oxidation of a wide range of terminal olefins to the corresponding methyl ketones in good to excellent yields in acetonitrile. The catalytic reaction is proposed to proceed via *syn*–peroxypalladation and subsequent rate limiting 1,2–hydride shift, which is supported by kinetic studies. The electronic asymmetry of aPmic renders a well–defined coordination sphere at Pd. The favored arrangement of reactants on the metal center features an olefin *trans* to the pyridyl module and a ^{t}butylperoxide *trans* to the carbene. This arrangement gains added stability by the π–delocalization paved by the compatible orbitals on Pd, the pyridyl module and the olefin that is perpendicular to the Pd(aPmic) plane. The π–interactions are absent in an alternate arrangement wherein the olefin is *trans* to the carbene. DFT studies reveal the

matching orbital overlaps responsible for the preferred arrangement over the other. This work provides an orbital description for the electronic asymmetry of aPmic.

KEYWORDS: Electronically asymmetric ligands, annellated carbenes, mesoionic carbenes, Wacker–type oxidation, Catalysis.

INTRODUCTION

Electronically asymmetric ligands wherein the donor modules differ in their electronic characteristics have received significant attention in recent years.[1] The difference in electronic characteristics of the donor modules results in significant variation in the nature and strength of metal–ligand interactions. Electronic asymmetry of the pyridine–oxazoline ligand (Pyrox–A) (Scheme 1a) has been implicated in stabilizing low–valent Co(I) intermediates.[2] The electronic disparity also plays a key role in many transformations catalyzed by transition metal compounds by controlling the catalyst coordination sphere. For example, Pyrox–B (Scheme 1a) imparts site–selectivity in palladium–catalyzed 1,4–difunctionalization of isoprene by controlling the migratory insertion of alkene into the Pd–alkenyl bond.[3] Mechanistic studies suggested that the directed insertion is the result of the unique electronic asymmetry and steric properties of the ligand. Electronic asymmetry has also been found to influence the chiral induction in enantioselective transformations.[4] Based on density functional theory (DFT) calculations, Stahl and coworkers suggested that the electronic asymmetry of Pyrox–C (Scheme 1b) complements the steric asymmetry and thereby controls the stereochemical outcome of the amidopalladation step in the Pd(II)–catalyzed enantioselective oxidative amidation of alkenes.[4a]

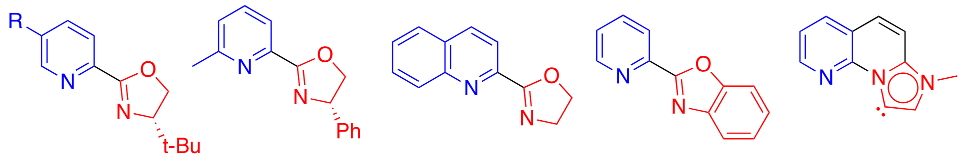

Pyrox (Sigman)
Pyrox-A (R = CN)
Pyrox-B (R = CF_3)
(a)

Pyrox-C (Stahl)
(b)

Quinox (Sigman)
(c)

Pyrbox (Muldoon)
(d)

aPmic (this work)
(e)

Scheme 1. Electronic asymmetric ligands.

Catalytic transformations that involve two electronically different reactants are best suited to evaluate the effects of electronic asymmetry of a ligand. In such transformations, the electronically asymmetric ligand directs the binding of the reactants (inner–sphere) in a specific arrangement. The most well–studied example is the catalyst–controlled Wacker–type oxidation, which involves the coordination of an olefin and a ^{t}butylperoxide to a Pd center. The Wacker oxidation is a synthetically important process for converting a terminal olefin to a methyl ketone.[5,6,7] Under Tsuji–Wacker conditions, this reaction is substrate controlled, which can result in a mixture of aldehyde and ketone products, especially when the alkene bears a proximal heteroatom.[1,8] Sigman and coworkers reported a Pd(II) compound featuring quinoline–2–oxazoline (Quinox) (Scheme 1c) for catalyzing the efficient and selective oxidation of difficult substrates such as allylic alcohols,[9a] internal olefins,[9b] protected allylic amines,[9c] and homoallylic alcohols[9d] employing ^{t}butylhydroperoxide (TBHP) as the oxidant. The excellent activity and selectivity of this catalyst were credited to the electronic disparity of the two coordinating modules of Quinox, featuring electron–rich oxazoline and electron–deficient quinoline rings.[10] Sigman hypothesized that ^{t}butylperoxide preferentially binds *trans* to oxazoline ring whereas alkene binds *trans* to quinoline ring (Scheme 2a). Hammett analysis of a series of substituted Quinox ligands revealed that the substitution by electron–withdrawing groups on quinoline ring enhanced the rate of the catalytic reactions.[10a] Similar inferences were also drawn by Hammett analysis of electronically diverse substrates. Muldoon group later examined 2–(2–pyridyl)benzoxazole (Pyrbox) (Scheme 1d) for the Pd catalyzed oxidation of terminal olefins to methyl ketones.[11] Notably, electronically symmetric ligand 2,2–bipyridine was ineffective in the catalytic oxidation of allylic acetate[9a,10a] and related catalytic reactions.[12,13,14]

One class of ligands which are particularly suitable to endure harsh conditions in oxidation chemistry is mesoionic carbenes (MICs).[15] Moreover, annellated carbenes exhibit unique stereoelectronic properties which can result in improved catalytic activity and selectivity of their metal complexes.[16] An annellated pyridyl–MIC (aPmic) ligand (Scheme 1e) was reported from our group for Ru(II) catalyzed selective C=C bond scission of olefins to aldehydes using $NaIO_4$ as oxidant at room temperature.[17] We now unravel the electronic asymmetric nature of aPmic in Pd–catalyzed Wacker–type oxidations. The two coordinating modules of this ligand differ in their relative ability for σ–donation/π–bonding. Whereas a carbene moiety is a strong σ–donor,[15] pyridyl unit exhibits π–bonding character besides acting as a σ–donor.[18] We reasoned that aPmic would impose a preferential binding of olefin and peroxide anion to Pd with respect to its electronically differentiated donor components (Scheme 2b). To validate this hypothesis, the catalytic activity of the Pd(II) complex **1** (Scheme 3) in Wacker–type oxidation of olefins to methyl ketones using TBHP as oxidant was examined. Very good efficiency and selectivity were observed for a wide range of olefins under optimized conditions. The catalytic reaction is proposed to proceed via *syn*–peroxypalladation and subsequent rate limiting 1,2–hydride shift, which is supported by kinetic studies. DFT calculations reveal that the key catalytically active species has a well–defined coordination of olefin and peroxide at Pd governed by the electronic asymmetry of aPmic. A delocalized π–bonding interaction is identified for the preferred orientation of olefin and peroxide anion with respect to the aPmic.

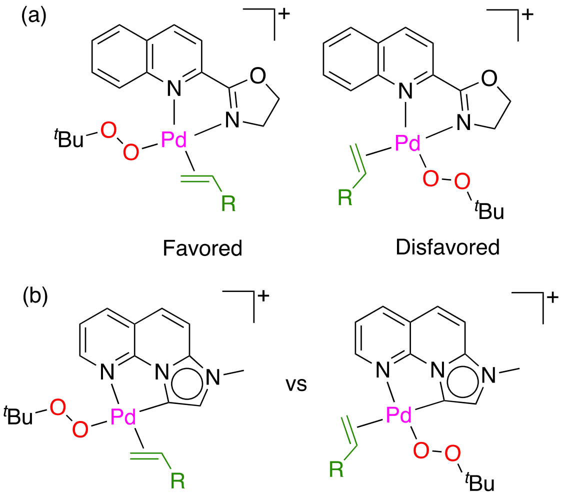

Scheme 2. Possible coordination models of Pd compounds featuring Quinox (a) and aPmic (b).

RESULT AND DISCUSSION

Synthesis of 1. Compound $[Pd(aPmic)(CH_3CN)_2][BF_4]_2$ (**1**) was obtained via the oxidative cleavage of the Pd–Pd bond in $[Pd_2(CH_3CN)_6][BF_4]_2$ with precursor salt in a dichloromethane/acetonitrile mixture at room temperature (Scheme 3).[19]

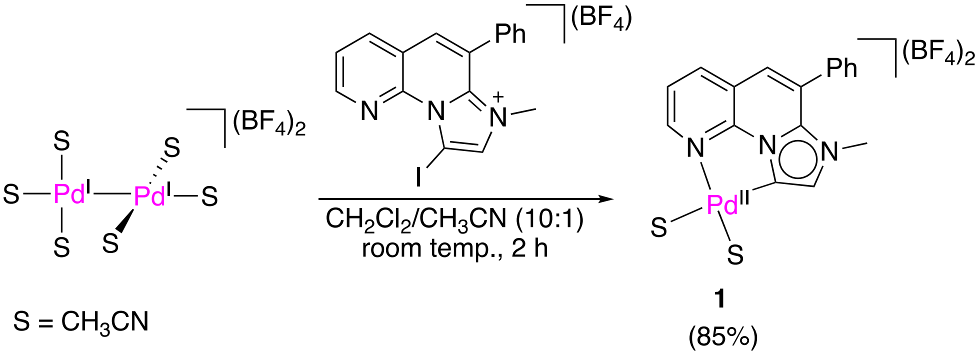

Scheme 3. Synthesis of compound **1**.

Catalytic Studies

Reaction Optimization. Initial experiment using styrene (1 mmol), TBHP(decane) (5 mmol) and catalyst **1** (0.05 mmol) in acetonitrile at 45 °C afforded a full conversion (100%) to acetophenone (entry 1, Table 1). The reduction of the catalyst loading and the amount of TBHP(decane) to 0.02 mmol and 3 mmol, respectively, did not alter the product amount and the selectivity for the model reaction (entry 2, Table 1). Further decrease in the amount of catalyst or oxidant, or lowering the temperature diminished the conversion as well as the selectivity. Screening of solvents and oxidants was carried out with the model reaction. Oxidants H_2O_2, $NaIO_4$ and O_2 were less efficient in terms of conversion and selectivity. Dichloromethane, tetrahydrofuran, dimethyl sulfoxide, toluene and methanol were ineffective.[20]

A control reaction was carried out (styrene/**1**/TBHP(decane) = 1 mmol/0.02 mmol/3 mmol; 45 °C, CH_3CN = 4 mL) using 5 mmol of H_2O^{18}. GC–MS analysis revealed no ^{18}O incorporation in the product acetophenone confirming that the source of the oxygen atom is TBHP. Initial rates of the model reaction (styrene/**1**/TBHP(decane) = 1 mmol/0.05 mmol/5 mmol; 45 °C) were studied by adding 2 to 50 mmol of H_2O externally. It was observed that the rate of the reaction decreases with the increase in H_2O amount. The model reaction was also performed in the presence of TBHP(aqueous) instead of TBHP(decane). For TBHP(aqueous), the reaction practically ceased after 12 h with 80% conversion and a black solid, presumably that of metallic Pd, was observed in the reaction vessel.

Table 1. Reaction optimization.

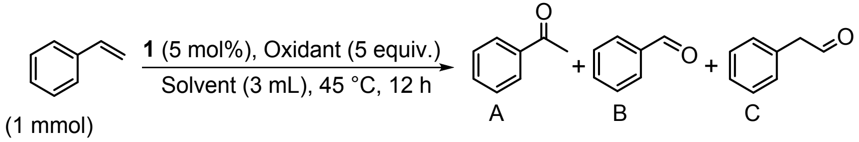

Entry	Oxidant	Solvent	Conv. (%)^a	A:B:C
1	TBHP(decane)	CH_3CN	100	99.99:0.01:0
2	TBHP(decane)^b	CH_3CN	98	99.99:0.01:0
3	H_2O_2(aq.)	CH_3CN	90	75:25:0
4	$NaIO_4$	CH_3CN/H_2O (2/1)	50	70:30:0
5	O_2^{c}	CH_3CN	30	0:100:0
6	TBHP(decane)	CH_2Cl_2	10	71:29:0
7	TBHP(decane)	THF	13	74:26:0
8	TBHP(decane)	DMSO	37	49:34:17
9	TBHP(decane)	Toluene	65	56:44:0
10	TBHP(decane)	MeOH	100	76:24:0

[a]Determined by GC–MS analysis using *n*–dodecane as an internal standard; [b]0.02 mmol of **1** and 3 mmol of oxidant used. [c]Schlenk vial was connected to a balloon containing molecular oxygen.

Substrate Scope. The substrate scope for catalyst **1** was explored under the following optimized reaction conditions: alkene/TBHP(decane)/**1** = 1 mmol/3 mmol/0.02 mmol; acetonitrile (4 mL); 45 °C (Table 2). Styrene, 4–methylstyrene, 3–methylstyrene and 2,4–dimethylstyrene afforded quantitative conversions to the corresponding methyl ketones (**1**–**4**). The presence of electron–donating groups –OMe/–SMe on the phenyl ring (4–methoxystyrene, 3,4–dimethoxystyrene and 4–methylthiostyrene) increased the reaction rate and full conversions to the corresponding products (**5**–**7**) were obtained within 4 h. The presence of electron–withdrawing groups, for examples, 4–fluorostyrene (72%, 30 h), 2–fluorostyrene (70%, 30 h) and 4–chlorostyrene (68%, 30 h) gave lower conversions to the corresponding methyl ketones (**8**–**10**). 2–vinylpyridine gave no product (**11**) presumably due to catalyst deactivation by coordination of the pyridine nitrogen to the metal center. Other heteroaromatic alkenes 1–methyl–2–vinyl–1H–pyrrole, 2–vinylfuran and 2,5–dimethyl–3–vinylthiophene gave the corresponding methyl ketones (**12**–**14**) in good yields. The oxidation of substrates having C=C bond attached to different polycyclic aromatic rings, such as, 2–vinylnaphthalene, 9–vinylanthracene and 1–vinylpyrene, afforded the corresponding methyl ketones (**15**–**17**) with 90–96% yields after 12 h. Vinylferrocene gave acetylferrocene (**18**) in 95% yield after 12 h.

Due to lower reactivity of the aliphatic alkenes in comparison to the aromatic congeners, the reactions of aliphatic alkenes were carried out with higher catalyst loading (5 mol%) and 5 equiv. of TBHP(decane) at 45 °C. The oxidation of aliphatic terminal alkenes afforded ~55% conversion after 36 h. However, increasing the temperature to 70°C led to considerably higher yields. Excellent yields of the corresponding products **19**–**22** were obtained for 2–allylisoindoline–1,3–dione (80%), vinylcyclohexane (90%), 4,4–dimethoxybut–1–ene (95%) and ethyl acrylate (85%) within 24 h.

Internal alkenes *trans*–stilbene and *cis*–stilbene afforded the product **23** in 50% and 56% conversions, respectively, after 36 h with ~5–10% benzaldehyde as the side product. At elevated temperature (70°C), *trans/cis*–stilbenes result in 82% and 85% conversions, respectively, after 24 h without any trace of benzaldehyde. Oxidation of *trans*–*β*–methylstyrene gave a mixture of products propiophenone (**24**) and phenylacetone (**25**) (70:30 ratio) after 24 h. Indene afforded 2–indanone (**26**) with 52% conversion after 36 h. Internal aliphatic alkene, *cis*–cyclooctene, also yielded 50% of cyclooctenone (**27**) after 36 h. Indene and *cis*–cyclooctene afforded 95% and 90% conversions, respectively, after 24 h at 70 °C.

Table 2. Substrate Scope.[a]

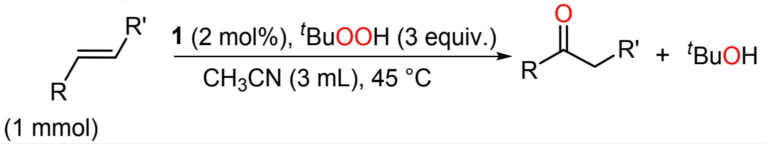

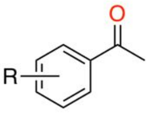

1[b] R = H (98%, 12 h)
2[b] R = 4–CH$_3$ (99%, 12 h)
3[b] R = 3–CH$_3$ (99%, 12 h)
4[b] R = 2,4–CH$_3$ (99%, 12 h)
5 R = 4–OCH$_3$ (100%, 4 h)
6 R = 3,4–OCH$_3$ (100%, 4 h)
7 R = 4–SCH3 (100%, 4 h)
8[b] R = 4–F (72%, 30 h)
9[b] R = 2–F (70%, 30 h)
10[b] R = 4–Cl (68%, 30 h)

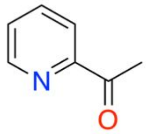

11 (0%, 12 h)

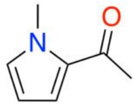

12[b] (90%, 12 h)

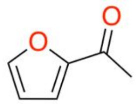

13[b] (90%, 12 h)

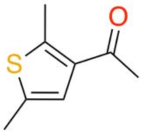

14[b] (92%, 12 h)

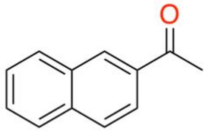

15[b] (96%, 12 h)

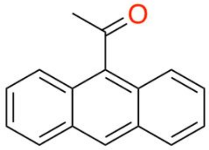

16[b] (90%, 12 h)

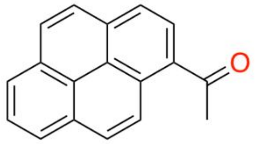

17[b](95%, 12 h)

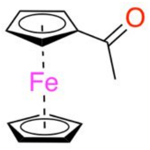

18[b] (95%, 12 h)

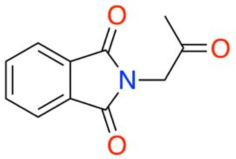

19[c](60%, 36 h)
(80%, 24 h)[d]

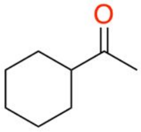

20[c] (50%, 36 h)
(90%, 24 h)[d]

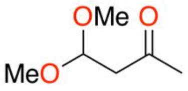

21[c] (55%, 36 h)
(95%, 24 h)[d]

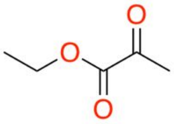

22[c] (60%, 36 h)
(85%, 24 h)[d]

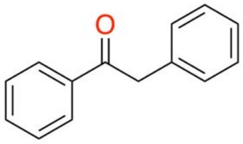

23[e] (50%, 36 h)[f,g]
(82%, 24 h)[d,f]
(56%, 36 h)[g,h]
(85%, 24 h)[d,h]

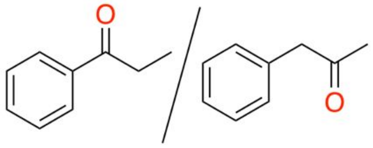

24+25 (70:30, 24 h)

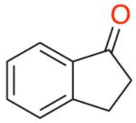

26[c] (52%, 36 h)
(95%, 24 h)[d]

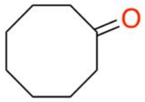

27[c,i] (50%, 36 h)
(90%, 24 h)[d]

[a]Yield was determined by GC–MS analysis using *n*–dodecane as an internal standard; [b]Traces of C=C cleaved product also detected; [c]catalyst **1** (0.05 mmol) and 5 mmol of TBHP(decane) used; [d]Reaction temperature: 70 °C; [e]Both *trans* and *cis*–stilbene gave the same product 1,2 diphenylethanone; [f]Using *trans*–Stilbene; [g]~5–10% benzaldehyde obtained; [h]Using *cis*–stilbene; [i]~2–3% epoxide.

An important advantage of this catalyst is that it does not require Ag salt to be active.[11] The bidentate aPmic ligand provides access to incoming oxidant and olefin in *cis* orientation by the removal of two acetonitriles. To investigate the fate of the catalyst, a stoichiometric reaction was performed with equimolar (0.1 mmol) amount of catalyst **1**, styrene and TBHP(decane) in acetonitrile. After 4 h, the solvent was evaporated, and the solid residue was washed with (3 × 10 mL) diethyl ether. It was then dissolved in acetonitrile and diethyl ether was layered to obtain crystals, which were collected, weighed (yield 72%) and identified to be the catalyst **1** by X–ray crystallography and ESI–MS. Recovery of the catalyst suggests that its molecular integrity is retained during the oxidation.

Ligand Asymmetry

For the oxidation reaction to proceed, one molecule each of olefin and ^{t}BuOO^{-} needs to bind the metal. An electronic asymmetric ligand enables the metal to bind the precursors in a specific arrangement. Thus, the binding of two olefins or two ^{t}BuOO^{-} to Pd center, which result in a catalytically inactive species, is averted. In Sigman's catalyst, the disparity in the binding of two reactants is caused by the presence of electron–poor quinoline ring and electron–rich oxazoline. ^{t}BuOO^{-} preferably binds *trans* to oxazoline and olefin binds the electrophilic site *trans* to quinoline. We argued that aPmic ligand may display electronic disparity due to the difference in the σ– and π–characteristics of its two donor modules (*vide infra*). Therefore, one could assume an arrangement where π–acid ligand olefin binds *trans* to the pyridyl unit and the σ–donor ^{t}BuOO^{-} binds *trans* to the carbene carbon which is also a σ–donor (Scheme 4). This matching arrangement is defined as ‘σσ/ππ’ whereas the reverse arrangement, where ^{t}BuOO$^-$ and olefin bind metal *trans* to the pyridyl and the carbene, respectively, is identified as ‘σπ/σπ’.[21]

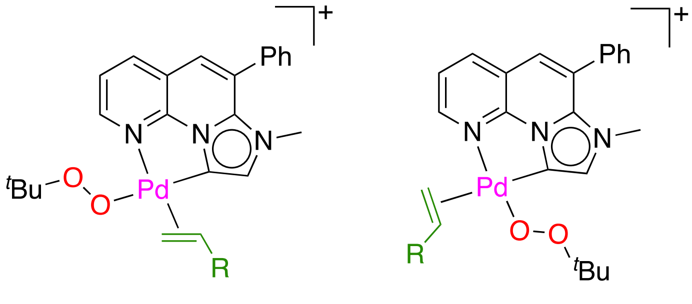

σσ/ππ (Match) σπ/σπ (Mismatch)

Scheme 4. Two possible arrangements for binding of ^{t}BuOO$^-$ and olefin.

Reaction Mechanism

A plausible mechanism for this TBHP–mediated Wacker oxidation, similar to the one proposed by Sigman[10] and Mimoun,[22] is depicted in Scheme 5. Initially, **1** reacts with olefin and ^{t}BuOOH to form species **A** with σσ/ππ arrangement. This is followed by *syn*–peroxypalladation involving nucleophilic attack of the coordinated oxygen atom of ^{t}BuOO$^-$ to the olefin, providing an intermediate **B**. To release the strain in the four–membered ring, intermediate **B** undergoes a rapid rearrangement affording the five–membered pseudo-palladacyclic species **C**. Heterolytic cleavage of the O–O bond with a concomitant 1,2–hydride shift gives intermediate **D**. Finally, the methyl ketone and ^{t}BuOH are released to complete the cycle.

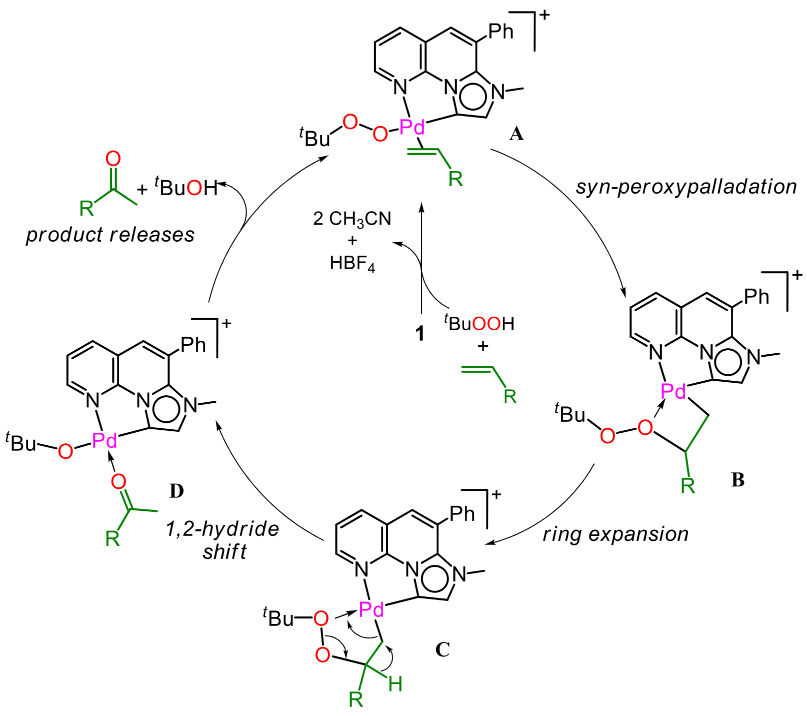

Scheme 5. Proposed mechanism for olefin oxidation by **1** (σσ/ππ).

Kinetic Studies

Kinetic studies are carried out to validate the proposed mechanism. The initial rate of the reaction was monitored (up to <10–15% conversion) to determine the reaction order with respect to the catalyst **1**, the alkene (styrene) and TBHP(decane). The initial rate varied linearly with [**1**] and [styrene] (Figures 1(a) and 1(b)). Increasing [TBHP(decane)] results in a faster rate, until a certain point. After that, increasing [TBHP] leads to no further acceleration of the reaction (Figure 1(c)). The saturation kinetics for [TBHP(decane)] and the first order dependency with respect to [styrene] indicates the coordination of TBHP before styrene.[10a]

The initial rates of the reactions of electronically varied *para*–substituted styrenes (*p*–$YC_6H_4CH{=}CH_2$; Y= OMe, Me, H, F, Cl) with '**1** + TBHP(decane)' were measured. The Hammett plot of log[initial rate] vs σ^+ (Hammett constant) gave a straight line with a ρ^+ value of –2.99 (see, SI). A negative ρ^+ value suggests the development of positive charge at the α–carbon atom of styrene implying that the rate of the reaction should be accelerated by electron–donating substituents. This is in agreement with the results discussed under substrate scope.

The proposed mechanism involves two key steps– *syn*–peroxypalladation and 1,2–hydride shift. A Lewis-acid/Lewis-base interaction between the cationic palladium and alkene in the formation for species **A** would be favored by an electron-donating group, which is in line with the experimental results.[10a] Further, palladation results in the development of positive charge at olefin and should be slowed by electron–withdrawing substituents.[23] For 1,2–hydride shift as well, an electron–withdrawing substituent would result in a slower rate due to decrease in electron density at the α-C atom. This is consistent with the Hammett studies.

The effect of temperature on the rate of the reaction of **1** with styrene was also examined. The activation parameters were determined from the plot of ln(k/T) versus 1/T, which was linear over the temperature range studied (308–333 K). The estimated entropy of activation ($\Delta S^{\ddagger}$) is –22.39 ± 0.48 cal mol^{-1} K^{-1} and the enthalpy of activation ($\Delta H^{\ddagger}$) is 11.76 ± 0.09 kcal mol^{-1}.[24] A negative $\Delta S^{\#}$ value is indicative of an organized transition state in the rate–limiting step.

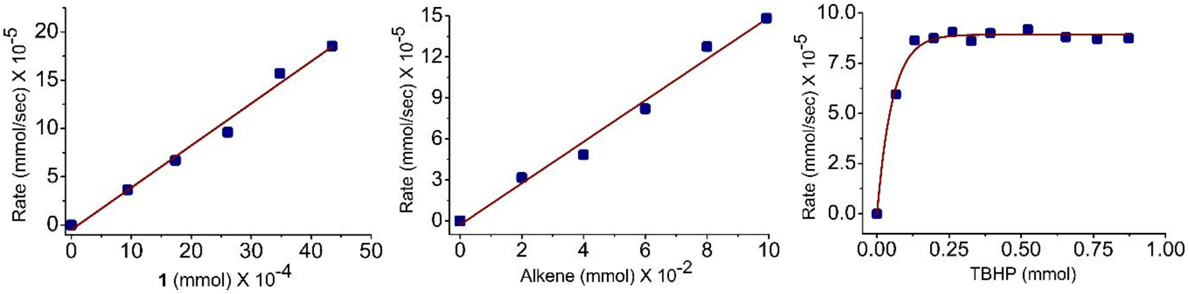

(a) (b) (c)

Figure 1. Initial rates *vs* (*a*) [**1**], (*b*) [alkene]; (*c*) [TBHP(decane)].

DFT Calculations

DFT calculations were carried out to distinguish between the catalytic cycles starting with species having σσ/ππ and σπ/σπ arrangements. The optimized structures of all intermediates and transition states along the match (σσ/ππ) and mismatch (σπ/σπ) pathways are provided in Figure 2 (σσ/ππ) and Figure S8 (σπ/σπ), respectively. The intermediates and transition states for σσ/ππ path are denoted by alphabets whereas the corresponding structures for σπ/σπ path are represented by the same alphabets with a prime symbol (′). A comparative energy profile is given in Figure 3. The calculations were carried at the M06 level of theory.[25] The basis set of Hay and Wadt (LanL2DZ) with effective core potential (ECP) was used for Pd.[26] Other atoms were described using the 6–31+G(d,p) basis set.[27] The technical details of the calculations are given in the SI.

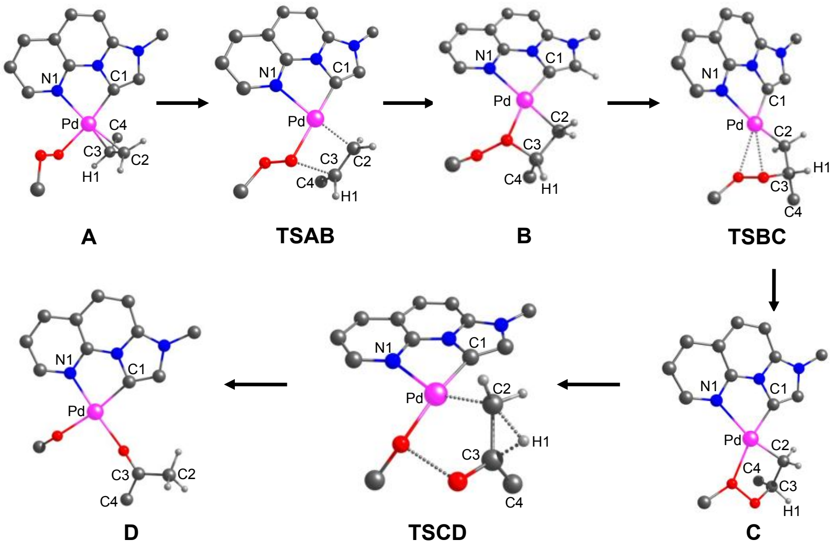

Figure 2. DFT optimized structures of all intermediates and transition states for olefin oxidation by **1** (σσ/ππ). Ph substituent on the ligand, H atoms (except on C2, C3) and Me groups of ^{t}Bu are removed for clarity.

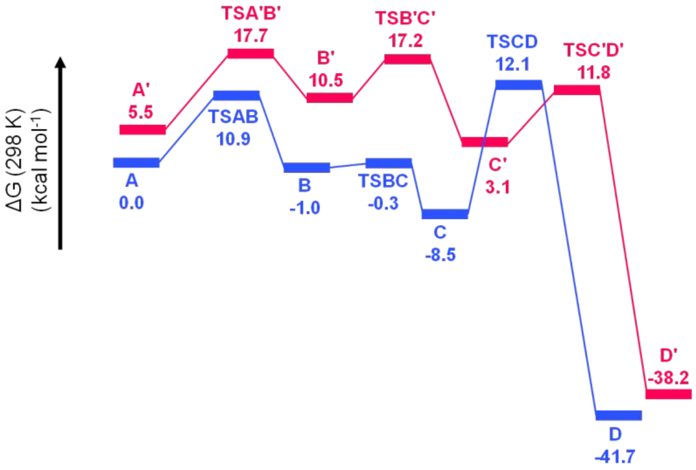

Figure 3. Free energy profiles of σσ/ππ (blue) and σπ/σπ (red) pathways are shown.

A careful comparison of the bond parameters of the computed structures reveal interesting features. The most notable difference in **A** and **A′** is the orientation of the olefin. The olefin is perpendicular to the Pd(aPmic) plane in **A** (Figure 4, the interplanar angle Φ = 70°), whereas it lies in the Pd(aPmic) plane in **A′** (Φ = 8°). The structure of **A** is akin to well–known Zeise's salt K[$PtCl_3(C_2H_4)$] where the olefin is disposed perpendicular to the $PtCl_3$ plane.[28] There are significant differences in the metrical parameters of **A** and **A′**. The olefin *trans* to pyridyl unit is more strongly bound to Pd (Pd–C2/C3 = 2.204/2.267 Å) in **A** than to the carbene (Pd–C2/C3 = 2.364/2.540 Å) in **A′**. The corresponding Pd–C2/C3 bond orders are 0.336/0.285 and 0.207/0.146, respectively. The C2–C3 distance is longer in **A** (1.380 Å) as compared to **A′** (1.355 Å). Accordingly, the C2–C3 bond order in **A** (1.567) is lesser than in **A′** (1.730). Interestingly, Pd–N1 distance (2.187 Å) is significantly shorter in **A** than in **A′** (2.255 Å), tallying with the calculated bond orders (0.299, 0.270). Pd–O1 distances in **A** (2.028 Å) and **A′** (2.011 Å) are similar. Pd–C1 distance in **A** (2.062 Å) differs slightly as compared to **A′** (2.013 Å). The favorable bonding situation in **A** aids to its stability by 5.5 kcal mol^{-1} than **A′** (*vide infra)*.

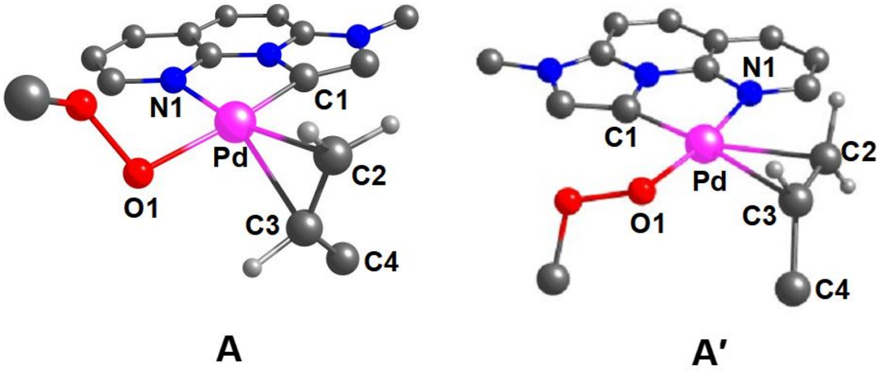

Pd-C2/C3 = 2.204/2.267, Pd–N1 = 2.187, C2–C3 = 1.380, Pd–O1 = 2.028, Pd–C1 = 2.061, Φ = 70.

Pd-C2/C3 =2.365/2.540, Pd–N1 = 2.255, C2–C3 = 1.355, Pd–O1 = 2.011, Pd–C1 = 2.013, Φ = 8.

Figure 4. Structures of **A** and **A′** with selected bond distances (Å) and interplanar angle Φ (°) given below. Ph, hydrogens (except on C2 and C3) and Me groups of ^{t}Bu are removed for clarity. Interplanar angle is the angle between Pd–C2–C3 and N1–Pd–C1 planes.

Metal-bound olefin is susceptible to the nucleophilic attack.[29] The *syn*–peroxypalladation step involves the nucleophilic attack of the coordinated oxygen atom of ^{t}BuOO^{-} to the olefin providing **B**. The free energy barrier for the formation of **B** (10.9 kcal mol^{-1}) is slightly less as compared to **B′** (12.2 kcal mol^{-1}). The Pd–C1(carbene) and Pd–C2(olefin) distances are shorter in **B** (1.994 and 2.036 Å) as compared to the same in **B′** (2.156 and 2.060 Å). **B′** is destabilized compared to **B** by 11.5 kcal mol^{-1}. A near barrier–less (0.7 kcal mol^{-1}) conversion of **B** to **C** releases the ring strain. The energy difference between **C** and **C′** was found practically identical (11.6 kcal mol^{-1}) to that of **B** and **B′**. The structural parameters of **C** and **C′** reflect the same pattern as that in **B** and **B′**. The next step involves heterolytic O–O bond cleavage with a concomitant 1,2–hydride shift that affords the product. The activation energy for this step is higher (20.6 kcal mol^{-1}) for σσ/ππ pathway compared to the alternate σπ/σπ pathway (8.7 kcal mol^{-1}).

The free energy difference between **A** and **A′** is reflective of the different ligand arrangements around the metal. Since **A** is stable than **A′**, the σσ/ππ pathway appears to be operational here. Furthermore, the free energy barriers show that 1,2–hydride shift (**C**→**D**) should be the rate–limiting step for the σσ/ππ pathway. Along the σπ/σπ pathway, the transition state corresponding to the peroxypalladation (**TSA′B′**) is located at the highest point in the energy landscape which contradicts with 1,2–hydride shift being the rate limiting step. Thus, the σπ/σπ cycle can be ruled out.

The preferential binding of reactants could be understood from a schematic orbital interaction diagram given in Figure 5.[30] The pyridine module guides the orientation of the olefin in **A**. A perpendicular arrangement of olefin to the Pd–pyridyl (aPmic) plane allows the overlap of *p*π orbital of N1, *d*π of Pd and π* of olefin establishing a π–corridor (Figure 5a). The Pd→C2–C3 π* (p_z–p_z) back–donation is enhanced by the filled-filled interaction of N1(p_y) with Pd (*d*π). Although pyridine is a weak π–donor, annellation with an electron–rich aromatic system likely improves the π–donicity of pyridyl module in aPmic. The enhanced Pd→π*(C2–C3) back–donation in **A** than **A′** is revealed by the natural bond orbital (NBO) analysis.[31] The second–order perturbation energy ($E^{(2)}$) corresponding to Pd→π*(C2–C3) is significantly higher in **A** (25.6 kcal mol^{-1}) than **A′** (8.7 kcal mol^{-1}).

A higher Pd→olefin back–bonding can augment σ–donation from N1(sp^2)→Pd(dz^2) which is responsible for shorter Pd–N1 distance. This is also reflected in $E^{(2)}$ corresponding to N1→Pd interaction which is higher in **A** (43.3 kcal mol^{-1}) than **A′** (27.4 kcal mol^{-1}). The σ–donation from C2–C3→Pd is also stronger in **A** than **A′** as revealed by the corresponding $E^{(2)}$ values (46.9 and 9.7 kcal mol^{-1}, respectively). Clearly, a π–corridor cannot be established if the C2–C3 axis lies in the Pd(aPmic) plane as N1(p_y) and C2–C3 π* would be mutually orthogonal. The efforts to optimize a related structure where C2–C3 axis resides in the Pd(aPmic) plane failed, instead, the structure of **A** was invariably obtained.

The aPmic ligand imposes a preference for olefin to bind the metal *trans* to pyridyl module and perpendicular to the Pd(aPmic) plane to pave the way for the π–corridor. The mutually *trans* ^{t}butylperoxide and carbene constitute a σ–framework (Figure 5b). The Pd–O1 distances are similar irrespective of its *trans* partners in **A** and **A′** indicating similar interactions of ^{t}butylperoxide with the metal.

Overall, the matching arrangement (**A**) has significant π–type interactions between *p*π of N1, *d*π of Pd and π* of olefin. In contrast, the pyridyl and olefin are not mutually *trans* and the π–

type interactions are absent in **A′**. Hence a perpendicular disposition of olefin is not warranted in **A′**. The *cis* Pd–N1 and Pd–C2/C3 interactions are thus weaker in comparison. The additional π–interactions in **A** incentivize the preference of the olefin and ^{t}butylperoxide anion to bind in a particular arrangement.

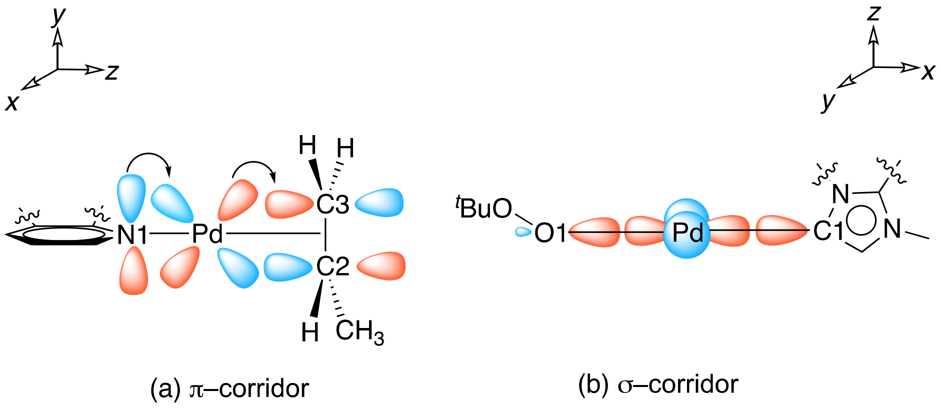

(a) π–corridor (b) σ–corridor

Figure 5. Schematic representations of the π– and σ–interactions involving N1(p_y), Pd(d_{yz}) and (C2–C3)(p_z–p_z)* orbitals (a) and O1(sp^2), Pd($d_{x^2-y^2}$) and C1(sp^2) orbitals (b), respectively, in matching arrangement **A**.

CONCLUSION

Herein we revealed the electronic asymmetry of bidentate annellated pyridyl–mesoionic carbene ligand (aPmic). The electronic asymmetry of aPmic originates from the difference in the σ– and π–bonding characteristics of its two donor modules. The aPmic ligand guides olefin to bind the metal *trans* to pyridyl module and perpendicular to the Pd(aPmic) plane to allow π–delocalization involving compatible orbitals on pyridyl module and olefin. The added stability associated with the π–delocalization imposes a preference for olefin, and thereby ^{t}butylperoxide, to bind the metal center in a particular arrangement. The rational based on the σ– and π–bonding properties of the donor modules outlined here provides an orbital perspective to Sigman's approach to electronic asymmetry. The aPmic was applied in the Pd(II) catalyzed Wacker type oxidation of terminal olefins as a proof of concept of its electronic asymmetry. This ligand may have wider utility in catalytic reactions involving electronically disparate substrates. We are currently working in this direction.

ASSOCIATED CONTENT

Supporting Information. Detailed experimental procedures, kinetic plots, supporting figures and computational details (PDF). The Supporting Information is available free of charge at https://pubs.acs.org/doi……..

AUTHOR INFORMATION

Corresponding Author

*jbera@iitk.ac.in

Notes

The authors declare no competing financial interest.

ACKNOWLEDGMENT

We thank the anonymous reviewers for insightful comments. We also thank Prof. Nisanth N. Nair and Prof. Ayan Datta for their valuable suggestions on this work. Financial support from the Science and Engineering Research Board (SERB), the Department of Atomic Energy (DAE), and the Indo−French Centre for the Promotion of Advanced Research (IFCPAR) are gratefully acknowledged. J.K.B. thanks SERB, India, for a J. C. Bose fellowship. S.S. and S.Y. thank the UGC, India, I.D. thanks the CSIR, India, for fellowships. N.U.D.R. thanks IIT Kanpur for a post–doctoral fellowship.

REFERENCES

(1) Sigman, M. S.; Werner, E. W. Imparting Catalyst Control upon Classical Palladium–Catalyzed Alkenyl C–H Bond Functionalization Reactions. *Acc. Chem. Res.* **2012**, *45*, 874–884.

(2) Hickey, D. P.; Sandford, C.; Rhodes, Z.; Gensch, T.; Fries, L. R.; Sigman, M. S.; Minteer, S. D. Investigating the Role of Ligand Electronics on Stabilizing Electrocatalytically Relevant Low–Valent Co (I) Intermediates. *J. Am. Chem. Soc.* **2019**, *141*, 1382–1392.

(3) McCammant, M. S.; Sigman, M. S. Development and investigation of a site selective palladium–catalyzed 1, 4–difunctionalization of isoprene using pyridine–oxazoline ligands. *Chem. Sci.* **2015**, *6*, 1355–1361.

(4) (a) McDonald, R. I.; White, P. B.; Weinstein, A. B.; Tam, C. P.; Stahl, S. S. Enantioselective Pd(II)–Catalyzed Aerobic Oxidative Amidation of Alkenes and Insights into the Role of Electronic Asymmetry in Pyridine–Oxazoline Ligands. *Org. Lett.* **2011**, *13*, 2830–2833. (b) Xu, J. Influence of the electronic effect of catalysts on the enantioselectivity: applicability and complexity. *Curr. Org. Synth.* **2010**, *7*, 650–676. (c) Armstrong, P. B.; Dembicer, E. A.; DesBois, A. J.; Fitzgerald, J. T.; Gehrmann, J. K.; Nelson, N. C.; Noble, A. L.; Bunt, R. C. Investigation of the Electronic Origin of Asymmetric Induction in Palladium–Catalyzed Allylic Substitutions with Phosphinooxazoline (PHOX) Ligands by Hammett and Swain–Lupton Analysis of the ^{13}C NMR Chemical Shifts of the (π–Allyl) palladium Intermediates. *Organometallics* **2012**, *31*, 6933–6946.

(5) For recent reviews, see (a) Baiju, T. V.; Gravel, E.; Doris, E.; Namboothiri, I. N. N. Recent Developments in Tsuji–Wacker Oxidation. *Tetrahedron Lett.* **2016**, *57*, 3993–4000. (b) Dong, J. J.; Browne, W.R.; Feringa, B. L. Palladium–Catalyzed anti–Markovnikov Oxidation of Terminal Alkenes. *Angew. Chem., Int. Ed.* **2015**, *54*, 734–744. (c) Mann, S. E.; Benhamou, L.; Sheppard, T. D. Palladium (II)–catalysed oxidation of alkenes. *Synthesis*, **2015**, *47*, 3079–3117. (d) Guo, J.; Teo, P. Anti–Markovnikov Oxidation and Hydration of Terminal Olefins. *Dalton Trans.* **2014**, *43*, 6952–6964. (e) Michael, B. W.; Sigman, M. S. Peroxide–Mediated Wacker Oxidations for Organic Synthesis. *Aldrichimica Acta* **2011**, *44*, 55–62. (f) Keith, J. A.; Henry, P. M. The Mechanism of the Wacker Reaction: A Tale of Two Hydroxypalladations. *Angew. Chem., Int. Ed.* **2009**, *48*, 9038–9049. (g) Jira R. Acetaldehyde from ethylene–A Retrospective on the Discovery of the Wacker Process. *Angew. Chem., Int. Ed*. **2009**, 48, 9034–9037. (h) Cornell, C. N.; Sigman, M. S. Recent Progress in Wacker Oxidations: Moving toward Molecular Oxygen as the Sole Oxidant. *Inorg. Chem.* **2007**, *46*, 1903–1909. (i) Muzart, J. Aldehydes from Pd–Catalyzed Oxidation of Terminal Olefins. *Tetrahedron* **2007**, *63*, 7505–7521. (j) Takacs, J.; Jiang, X. The Wacker Reaction and Related Alkene Oxidation Reactions. *Curr. Org. Chem.* **2003**, *7*, 369–396. (k) Tsuji, J. Organopalladium Chemistry in the ’60s and ’70s. *New J. Chem.* **2000**, *24*, 127–135. (l) Tsuji, J. Recollections of Organopalladium Chemistry. *Pure Appl. Chem.* **1999***, 71,* 1539–1547.

(6) For synthetic applications, see (a) Tamiya, M.; Isaka, N.; Kitazawa, T.; Hasegawa, A.; Ishizawa, K.; Ikeda, M.; Kawada, S.; Ishiguro, M. Total Syntheses of the Non–peptide Bradykinin B1 Receptor Antagonist Velutinol A and its Analogs, seco–Pregnanes with a Cage–like Moiety. *Bull. Chem. Soc. Jpn*. **2019**, *92*, 1474–1494. (b) Total Synthesis of 2–(2–Ketoalkyl)–piperidine Alkaloids (+) Pelletierine, (+)–Haloxynine and (-)–*N*-Methyl–pelletierine via Regioselective Wacker Oxidation *ChemistrySelect*, **2019**, *4*, 8564–8567. (c) Niesobski, P.; Martínez, I. S.; Kustosz, S.; Müller, T. J. Sequentially Pd/Cu–Catalyzed Alkynylation–Oxidation Synthesis of 1,2–Diketones and Consecutive One–Pot Generation of Quinoxal. Eur. J. Org. Chem. **2019**, *31–32*, 5214–5218. (d) Ramakrishna, G. V.; Fernandes, R. A. Total Synthesis of the Sensitive Triyne Natural Product (4 S ,5 S)–4,8–Dihydroxy–3,4–Dihydrovernoniyne and All of Its Stereoisomers. *Org. Lett.* **2019**, *21*, 5827–5831. (e) Sun, W.; Zhang, M.; Li, P.; Li, Y. One–Pot Synthesis of Polysubstituted Imidazoles Based on $Pd(OAc)_2/Ce(SO_4)_2/Bi(NO_3)_3$ Trimetallic Cascade of Decarboxylation/Wacker–Type Oxidation/Debus–Radziszewski Reaction. *Synthesis (Stuttg).* **2019**, *51*, 3221–3230. (f) González–Martínez, D.; Gotor, V.; Gotor–Fernández, V. Stereoselective Synthesis of 1–Arylpropan–2–Amines from Allylbenzenes through a Wacker–Tsuji Oxidation–Biotransamination Sequential Process. *Adv. Synth. Catal.* **2019**, *361*, 2582–2593. (g) Steib, P.; Breit, B. Concise Total Synthesis of (−)–Vermiculine through a Rhodium–Catalyzed C 2–Symmetric Dimerization Strategy. *Chem. – A Eur. J.* **2019**, *25*, 3532–3535. (h) Luu, H. T.; Streuff, J. Development of an Efficient Synthesis of Rac–3–Demethoxyerythratidinone via a Titanium(III) Catalyzed Imine–Nitrile Coupling. *Eur. J. Org. Chem.* **2019**, *2019*, 139–149. (i) Smith, C. D.; Phillips, D.; Tirla, A.; France, D. J. Catalytic Isohypsic–Redox Sequences for the Rapid Generation of Csp3–Containing Heterocycles. *Chem. – A Eur. J.* **2018**, *24*, 17201–17204. (j) Wachtendorf, D.; Geibel, I.; Schmidtmann, M.; Christoffers, J. Octahydrocyclopenta[c]Pyridine Scaffold – Enantioselective Synthesis and Indole Annulation. *European J. Org. Chem.* **2018**, *2018*, 5524–5531. (k) Yan, J. L.; Cheng, Y.; Chen, J.; Ratnayake, R.; Dang, L. H.; Luesch, H.; Guo, Y.; Ye, T. Total Synthesis of Asperphenins A and B. *Org. Lett.* **2018**, *20*, 6170–6173. (l) Von Czapiewski, M.; Rhein, M.; Meier, M. A. R. Fatty Acid Derived Renewable Platform Chemicals via Selective Oxidation Processes. *ACS Sustain. Chem. Eng.* **2018**, *6*, 15170–15179. (m) Liu, Y.; Zhang, Y.; Wang, X.; Fu, S.; Liu, B. Synthesis of Polycyclic Frameworks through Iron–Catalyzed

Intramolecular [5+2] Cycloaddition. *Synlett* **2018**, *29*, 1978–1982. (n) Puls, F.; Kataeva, O.; Knölker, H. J. Synthesis of Euchrestifoline Using Iron– and Palladium–Catalyzed C–H Bond Activations. *European J. Org. Chem.* **2018**, 4272–4276. (o) Uthoff, F.; Gröger, H. Asymmetric Synthesis of 1–Phenylethylamine from Styrene via Combined Wacker Oxidation and Enzymatic Reductive Amination. *J. Org. Chem.* **2018**, *83*, 9517–9521. (p) Kommera, R.; Kasireddy, V. R.; Ghojala, V. R.; Bekkam, M.; Rebelli, P.; Yerrabelly, J. R. A Scalable Approach for the Synthesis of Epothilone Thiazole Fragment (C12–C21 Unit) Via Wacker Oxidation. *Synlett* **2018**, *29*, 1076–1078. (q) Pandey, K.; Rangan, K.; Kumar, A. One–Pot Tandem Amidation, Knoevenagel Condensation, and Palladium–Catalyzed Wacker Type Oxidation/C–O Coupling: Synthesis of Chromeno–Annulated Imidazopyridines. *J. Org. Chem.* **2018**, *83*, 8026–8035. (r) Uthoff, F.; Sato, H.; Gröger, H. Formal Enantioselective Hydroamination of Non–Activated Alkenes: Transformation of Styrenes into Enantiomerically Pure 1–Phenylethylamines in Chemoenzymatic One–Pot Synthesis. *ChemCatChem* **2017**, *9*, 555–558. (s) Liu, X.; Hu, Y. J.; Chen, B.; Min, L.; Peng, X. S.; Zhao, J.; Li, S.; Wong, H. N. C.; Li, C. C. Asymmetric Total Syntheses of Colchicine, β–Lumicolchicine, and Allocolchicinoid N–Acetylcolchinol–O–Methyl Ether (NCME). *Org. Lett.* **2017**, *19*, 4612–4615. (t) Kashinath, K.; Jachak, G. R.; Athawale, P. R.; Marelli, U. K.; Gonnade, R. G.; Srinivasa Reddy, D. Total Synthesis of the Marine Natural Product Solomonamide B Necessitates Stereochemical Revision. *Org. Lett.* **2016**, *18*, 3178–3181.

(7) For other recent examples, see: (a) Runeberg, P. A.; Eklund, P. C. Tsuji–Wacker–Type Oxidation beyond Methyl Ketones: Reacting Unprotected Carbohydrate–Based Terminal Olefins through the "Uemura System" to Hemiketals and α,β–Unsaturated Diketones. *Org. Lett.* **2019**, *21*, 8145–8148. (b) Gao, S.; Ma, Y.; Chen, W.; and Luo, J. Pd–Catalyzed Oxidation of Aldimines to Amides. *Synlett* **2018**, *29*, 2191–2194. (c) Carlson, A. S.; Calcanas, C.; Brunner, R. M.; Topczewski, J. J. Regiocontrolled Wacker Oxidation of Cinnamyl Azides. *Org. Lett*. **2018**, *20*, 1604–1607. (d) Corless, V. B.; Holownia, A.; Foy, H.; Mendoza–Sanchez, R.; Adachi, S.; Dudding, T.; Yudin, A. K. Synthesis of α–borylated Ketones by Regioselective Wacker Oxidation of Alkenylboronates. *Org. Lett.* **2018**, *20*, 5300–5303. (e) Hu, K. F.; Ning, X. S.; Qu, J. P.; Kang, Y.B. Tuning Regioselectivity of Wacker Oxidation in One Catalytic System: Small Change Makes Big Step. *J. Org. Chem*. **2018***, 83*, 11327–11332. (f) Liu, B.; Jin, F.; Wang, T.; Yuan, X.; Han, W. Wacker–Type

Oxidation Using an Iron Catalyst and Ambient Air: Application to Late–Stage Oxidation of Complex Molecules. *Angew. Chem., Int. Ed.* **2017**, *56*, 12712–12717. (g) Chu, C. K.; Ziegler, D. T.; Carr, B.; Wickens, Z. K.; Grubbs, R. H. Direct Access to β–Fluorinated Aldehydes by Nitrite–Modified Wacker Oxidation. *Angew. Chem., Int. Ed.* **2016**, *55*, 8435–8439. (h) Nakaoka, S.; Murakami, Y.; Kataoka, Y.; Ura, Y. Maleimide–Assisted Anti–Markovnikov Wacker–Type Oxidation of Vinylarenes Using Molecular Oxygen as a Terminal Oxidant. *Chem. Commun.* **2015**, *52*, 335–338. (i) Wickens, Z. K.; Skakuj, K.; Morandi, B.; Grubbs, R. H. Catalyst–Controlled Wacker–Type Oxidation: Facile Access to Functionalized Aldehydes. *J. Am. Chem. Soc.* **2014**, *136*, 890–893. (j) Lerch M. M; Morandi B; Wickens Z. K; Grubbs R. H. Rapid Access to β–Trifluoromethyl–Substituted Ketones: Harnessing Inductive Effects in Wacker–Type Oxidations of Internal Alkenes. *Angew. Chem., Int. Ed*. **2014**, *53*, 8654–8658. (k) Morandi, B.; Wickens, Z. K.; Grubbs, R. H. Practical and General Palladium–Catalyzed Synthesis of Ketones from Internal Olefins. *Angew. Chem., Int. Ed*. **2013**, *52*, 2944–2948. (l) Bourne, S. L.; Ley, S. V. A Continuous Flow Solution to Achieving Efficient Aerobic Anti–Markovnikov Wacker Oxidation. *Adv. Synth. Catal.* **2013**, *355*, 1905–1910. (m) Dong, J. J.; Fañanás–Mastral, M.; Alsters, P. L.; Browne, W. R.; Feringa, B. L. Palladium–Catalyzed Selective Anti–Markovnikov Oxidation of Allylic Esters. *Angew. Chem., Int. Ed.* **2013**, *52*, 5561–5565. (n) Zhang, G.; Xie, X.; Wang, Y.; Wen, X.; Zhao, Y.; Ding, C. Highly Selective Wacker Reaction of Styrene Derivatives: A Green and Efficient Aerobic Oxidative Process Promoted by Benzoquinone/$NaNO_2$/$HClO_4$ under Mild Conditions. *Org. Biomol. Chem.* **2013**, *11*, 2947–2950. (o) Wickens, Z. K.; Morandi, B.; Grubbs, R. H. Aldehyde–Selective Wacker–Type Oxidation of Unbiased Alkenes Enabled by a Nitrite Co–Catalyst. *Angew. Chem., Int. Ed.* **2013**, *52*, 11257–11260 (p) Teo, P.; Wickens, Z. K.; Dong, G.; Grubbs, R. H. Efficient and Highly Aldehyde Selective Wacker Oxidation. *Org. Lett.* **2012**, *14*, 3237–3239. (q) Choi, P. J.; Sperry, J.; Brimble, M. A. Heteroatom–Directed Reverse Wacker Oxidations. Synthesis of the Reported Structure of (–)–Herbaric Acid. *J. Org. Chem.* **2010**, *75*, 7388–7392. (r) Ren, W.; Xia, Y.; Ji, S. J.; Zhang, Y.; Wan, X.; Zhao, J. Wacker–Type Oxidation of Alkynes into 1, 2–Diketones Using Molecular Oxygen. *Org. Lett.* **2009**, *11*, 1841–1844. (s) Weiner, B.; Baeza, A.; Jerphagnon, T.; Feringa, B. L. Aldehyde Selective Wacker Oxidations of Phthalimide Protected Allylic Amines: A New Catalytic Route to B3–Amino Acids. *J. Am. Chem. Soc.* **2009**, *131*, 9473–9474. (t) Wang, J.

L.; He, L. N.; Miao, C. X.; Li, Y. N. Ethylene Carbonate as a Unique Solvent for Palladium–Catalyzed Wacker Oxidation Using Oxygen as the Sole Oxidant. *Green Chem.* **2009**, *11*, 1317–1320. (u) Speziali, M. G.; Costa, V. V.; Roles–Dutenhefner, P. A.; Gusevskaya, E. V. Aeroic Palladium(II)/Copper(II)–Catalyzed Oxidation of Olefins under Chloride–Free Nonacidic Conditions. *Organometallics* **2009**, *28*, 3186–3192. (v) Weiner, B.; Baeza, A.; Jerphagnon, T.; Feringa, B. L. *J. Am. Chem. Soc*. **2009**, *131*, 9473–9474. (w) Friestad, G. K.; Jiang, T.; Mathies, A. K. Aldehyde–Selective Wacker Oxidation in a Thiyl–Mediated Vinyl Group Transfer Route to Daunosamine. *Org. Lett.* **2007**, *9*, 777–780.

(8) For traditional Wacker–Tsuji conditions, see: (a) Tsuji, J. Synthetic Applications of the Palladium–Catalyzed Oxidation of Olefins to Ketones. *Synthesis* **1984**, 369–384. (b) Tsuji, J.; Nagashima, H.; Nemoto, H. A General Synthetic Method for the Preparation of Methyl Ketones from Terminal Olefins: 2–Decanone. *Org. Synth*. **1984**, 62, 9–13. (c) Clement, W. H.; Selwitz, C. M. Improved Procedures for Converting Higher α–Olefins to Methyl Ketones with Palladium Chloride. *J. Org. Chem*. **1964**, *29*, 241–243. (d) Smidt, J.; Hafner, W.; Jira, R.; Sieber, R.; Sedlmeier, J.; Sabel, A. Olefinoxydation mit Palladiumchlorid–Katastatoren. *Angew. Chem.* **1962**, *74*, 93–102.

(9) (a) Michel, B. W.; Camelio, A. M.; Cornell, C. N.; Sigman, M. S. A General and Efficient Catalyst System for a Wacker–Type Oxidation Using TBHP as the Terminal Oxidant: Application to Classically Challenging Substrates. *J. Am. Chem. Soc.* **2009**, *131*, 6076–6077. (b) Deluca, R. J.; Edwards, J. L.; Steffens, L. D.; Michel, B. W.; Qiao, X.; Zhu, C.; Cook, S. P.; Sigman, M. S. Wacker–Type Oxidation of Internal Alkenes Using Pd(Quinox) and TBHP. *J. Org. Chem.* **2013**, *78*, 1682–1686. (c) Michel, B. W.; McCombs, J. R.; Winkler, A.; Sigman, M. S. Catalyst–Controlled Wacker–Type Oxidation of Protected Allylic Amines. *Angew. Chem., Int. Ed.* **2010**, *49*, 7312–7315. (d) McCombs, J. R.; Michel, B. W.; Sigman, M. S. Catalyst–Controlled Wacker–Type Oxidation of Homoallylic Alcohols in the Absence of Protecting Groups. *J. Org. Chem.* **2011**, *76*, 3609–3613.

(10) (a) Michel, B. W.; Steffens, L. D.; Sigman, M. S. On the Mechanism of the Palladium–Catalyzed Tert–Butylhydroperoxide–Mediated Wacker–Type Oxidation of Alkenes Using Quinoline–2–Oxazoline Ligands. *J. Am. Chem. Soc.* **2011**, *133*, 8317–8325. (b) Cornell, C. N; Sigman, M. S. Discovery of and Mechanistic Insight into a Ligand–Modulated

Palladium–Catalyzed Wacker Oxidation of Styrenes Using TBHP. *J. Am. Chem. Soc.* **2005**, *1279*, 2796–2797.

(11) (a) Chai, H.; Cao, Q.; Dornan, L. M.; Hughes, N. L.; Brown, C. L.; Nockemann, P.; Li; J. Muldoon, M. J. Cationic Palladium (II) Complexes for Catalytic Wacker–Type Oxidation of Styrenes to Ketones Using O_2 as the Sole Oxidant. *Eur. J. Inorg. Chem*, **2017**, 5604–5608. (b) Cao, Q.; Bailie, D. S.; Fu, R.; Muldoon, M. J. Cationic Palladium(II) Complexes as Catalysts for the Oxidation of Terminal Olefins to Methyl Ketones Using Hydrogen Peroxide. *Green Chem.* **2015**, *17*, 2750–2757.

(12) For examples of oxidative coupling see: (a) White, P. B.; Jaworski, J. N.; Zhu, G. H.; Stahl, S. S. Diazafluorenone–Promoted Oxidation Catalysis: Insights into the Role of Bidentate Ligands in Pd–Catalyzed Aerobic Aza–Wacker Reactions. *ACS Catal.* **2016**, *65*, 3340–3348. (b) Ying, C. H.; Yan, S. B.; Duan, W. L. 2–Hydroxy–1, 10–phenanthroline vs 1, 10–phenanthroline: significant ligand acceleration effects in the palladium–catalyzed oxidative Heck reaction of arenes. *Org. Lett.* **2014***, 162,* 500–503. (c) Izawa, Y.; Stahl, S. S. Aerobic Oxidative Coupling of *o*-Xylene: Discovery of 2–Fluoropyridine as a Ligand to Support Selective Pd–Catalyzed C–H Functionalization. *Adv. Synth. Catal.* **2010**, *352*, 3223–3229. (d) Andappan, M. M.; Nilsson, P.; Larhed, M. The First Ligand–modulated Oxidative Heck Vinylation. Efficient Catalysis with Molecular Oxygen as Palladium (0) Oxidant. *Chem. Commun.* **2004**. *2*, 218–219.

(13) For oxidation of alcohols, see: (a) Nishimura, T.; Onoue, T.; Ohe, K.; Uemura, S. Palladium (II)–catalyzed Oxidation of Alcohols to Aldehydes and Ketones by Molecular Oxygen. *J. Org. Chem.* **1999**, *6418*, 6750–6755. (b) Nishimura, T.; Onoue, T.; Ohe, K.; Uemura, S. $Pd(OAc)_2$–catalyzed oxidation of alcohols to aldehydes and ketones by molecular oxygen. *Tetrahedron Lett.* **1998**, *39*, 6011–6014.

(14) Hubert, M.; Charpentier, R.; Mitschler, A. A.; Fischer, J.; Weiss, R.; Mimoun, H.; Weiss, R.; Charpentier, R.; Fischer, J. Palladium(II) Tert–Butyl Peroxide Carboxylates. New Reagents for the Selective Oxidation of Terminal Olefins to Methyl Ketones. The Role of Peroxymetalation in Selective Oxidative Processes. *J. Am. Chem. Soc.* **1980**, *102*, 1047–1054.

(15) (a) Vivancos, A.; Segarra, C.; Albrecht, M. Mesoionic and related less heteroatom stabilized N–heterocyclic carbene complexes: Synthesis, catalysis, and other applications. *Chem. Rev.*

2018, *118*, 9493−9586. (b) Crabtree, R. H. Abnormal, mesoionic and remote N–heterocyclic carbene complexes. *Coord. Chem. Rev.* **2013**, *257*, 755–766. (c) Krüger, A.; Albrecht, M. Abnormal N–heterocyclic carbenes: More than just exceptionally strong donor ligands. *Aust. J. Chem.* **2011**, *64*, 1113–1117. (d) Schuster, O.; Yang, L.; Raubenheimer, H. G.; Albrecht, M. Beyond conventional N–heterocyclic carbenes: abnormal, remote, and other classes of NHC ligands with reduced heteroatom stabilization. *Chem. Rev.* **2009**, *109*, 3445–3478.

(16) Reshi, N. D.; Bera, J. K. Recent advances in annellated NHCs and their metal complexes. *Coord. Chem. Rev.* **2020**, *422*, 213334.

(17) Daw, P.; Petakamsetty, R.; Sarbajna, A.; Laha, S.; Ramapanicker, R.; Bera, J. K. A Highly Efficient Catalyst for Selective Oxidative Scission of Olefins to Aldehydes: Abnormal–NHC–Ru(II) Complex in Oxidation Chemistry. *J. Am. Chem. Soc.* **2014**, *136*, 13987–13990.

(18) (a) Leyssens, T.; Peeters, D.; Orpen, A. G.; Harvey, J. N. How Important Is Metal–Ligand Back–Bonding toward YX_3 Ligands (Y = N, P, C, Si)? An NBO Analysis. *Organometallics* **2007**, *26*, 2637–2645. (b) Shepherd, R. E.; Proctor, A.; Henderson, W. W.; Myser, T. K. Assessment of the π–Acceptor Capability of Selected Ligands Based on the Photoelectron Spectra of Ruthenium Ammine Complexes. *Inorg. Chem.* **1987**, *26*, 2440–2444. (c) Nelson, S. M.; Shepherd, T. M. Metal–to–Ligand π–Bonding in Some Nickel(II) Pseudo–Halide Complexes with Heterocyclic Aromatic Amines. *Inorg. Chem.* **1965**, *4*, 813–817.

(19) Saha, S.; Daw, P.; Bera, J. K. Oxidative Route to Abnormal NHC Compounds from Singly Bonded [M–M] (M = Ru, Rh, Pd) Precursors. *Organometallics* **2015**, *34*, 5509–5512.

(20) Catalyst **1** decomposes in halogenated solvents and has limited solubility in toluene and THF. A related mixed aPmic/phosphine complex shows enhanced stability in dichloromethane (manuscript under revision). The poor activity/selectivity obtained in these solvents is likely due to the limited solubility and/or stability of the catalyst.

(21) Carbene and *t*BuOO⁻ anion are σ–donors. Olefin is a π–acceptor in addition to being a σ–donor. Annellated pyridine module, although predominantly a σ–donor exhibits π–bonding character. Accordingly, the arranagement where ^{t}BuOO⁻ and olefin bind *trans* to carbene and pyridine modules is defined as σσ/ππ.

(22) (a) Roussel, M.; Mimoun, H. Palladium–Catalyzed Oxidation of Terminal Olefins to Methyl Ketones by Hydrogen Peroxide. *J. Org. Chem*. **1980**, 45, 5387–5390. (b) Mimoun, H.; Perez

Machirant, M. M.; Seree de Roch, I. Activation of Molecular Oxygen: Rhodium–Catalyzed Oxidation of Olefins. *J. Am. Chem. Soc*. **1978**, 100, 5437–5444. (c) Igersheim, F.; Mimoun, H. Activation and Transfer of Molecular Oxygen. Oxidation of Terminal Olefins to Methyl Ketones by Rhodium Dioxygen Complexes. *J. Chem. Soc., Chem. Commun*. **1978**, 559–560. (d) Nishimura, T.; Kakiuchi, N.; Onoue, T.; Ohe, K.; Uemura, S. Palladium(II)–Catalyzed Oxidation of Terminal Alkenes to Methyl Ketones Using Molecular Oxygen. *J. Chem. Soc., Perkin Trans. 1*. **2000**, *12,* 1915–1918.

(23) The development of positive charge at olefin moiety in **TSAB** was confirmed by charge analysis (see, Table S2). In addition, DFT calculations with propene and 3-chloropropene showed that an electron withdrawing substituent increases the free energy barrier for both steps **A→B** and **C→D** by a similar margin (see, Tables S3).

(24) The measured thermodynamic parameters are comparable to computed values (see, Table S4).

(25) Zhao, Y.; Truhlar, D. G. The M06 suite of density functionals for main group thermochemistry, thermochemical kinetics, noncovalent interactions, excited states, and transition elements: two new functionals and systematic testing of four M06–class functionals and 12 other functionals. *Theor. Chem. Acc.* **2008***, 120*, 215–241.

(26) Hay, P. J.; Wadt, W. R. Ab initio effective core potentials for molecular calculations. Potentials for K to Au including the outermost core orbitals. *J. Chem. Phys.* **1985**, *82*, 299–310.

(27) (a) Hehre, W. J.; Ditchfield R.; Pople, J. A. Self–Consistent Molecular Orbital Methods. 12. Further extensions of Gaussian–type basis sets for use in molecular–orbital studies of organic–molecules. *J. Chem. Phys*. **1972**, *56*, 2257–2261. (b) Petersson, G. A.; Al–Laham, M. A. A complete basis set model chemistry. II. Open–shell systems and the total energies of the first–row atoms. *J. Chem. Phys*. **1991**, 94, 6081–6090.

(28) (a) Black, M.; Mais, R. H. B; Owston, P. G. The crystal and molecular structure of Zeise's salt K.$PtCl_3$.C_2H_4. *Acata Cryst*. **1969**, B25, 1753–1759. (b) Love, R. A.; Koetzle, T. F.; Williams, G. J.; Andrews, L. C.; Bau, R. Neutron diffraction study of the structure of Zeise's salt, $KPtCl_3(C_2H_4).H_2O$. *Inorg. Chem*. **1975**, *14*, 2653–2657. (c) Hajime, K. The Electronic Structure of Zeise's Salt, $[PtCl_3C_2H_4]^-$. *B. Chem. Soc. Jpn.* **1971**, *44*, 348–354. (d) For

translation of Zeise's original paper, see *Classics in Coordination Chemistry: Part 2*; Kauffman, G., Ed; Dover: New York, **1976**; 21–37.

(29) When coordinated to a metal, the olefin becomes susceptible to nucleophilic attack unlike free olefin which undergoes electrophilic attack. For a further discussion on this reversal (umpolung) see: Crabtree, R. H. *The Organometallic Chemistry of the Transition Metals*; Wiley: New York, **1988**, 91.

(30) To view the π–corridor, N1–Pd axis (Z-axis) is kept horizontal. Pd(aPmic) is in XZ plane perpendicular to olefin C2–C3 axis (Y-axis). For clarity, the σ–corridor is also shown horizontally.

(31) (a) Reed, A. E., Curtiss, L. A.; Weinhold, F. Intermolecular interactions from a natural bond orbital, donor–acceptor viewpoint. *Chem. Rev.* **1988**, *88*, 6, 899–926. (b) Weinhold, F.; Landis C. *Valency and Bonding: A Natural Bond Orbital Donor–Acceptor Perspective*; Cambridge University Press, **2005**, pp 363-575.

Table of Contents Graphic